Progress in Polymer Science xxx (2009) xxx–xxx

Contents lists available at ScienceDirect

Progress in Polymer Science

journal homepage: www.elsevier.com/locate/ppolysci

An overview on field-flow fractionation techniques and their applications in the separation and characterization of polymers

Fathi A. Messaud [a], Ron D. Sanderson [a,*], J. Ray Runyon [b], Tino Otte [c], Harald Pasch [c], S. Kim Ratanathanawongs Williams [b,**]

[a] *UNESCO Associated Centre for Macromolecules & Materials/Department of Chemistry & Polymer Science, University of Stellenbosch, Private Bag XI, Matieland 7602, South Africa*
[b] *Laboratory for Advanced Separations Technologies, Department of Chemistry and Geochemistry, Colorado School of Mines, Golden, CO 80401, USA*
[c] *German Institute for Polymers, Schlossgartenstr. 6, 64289 Darmstadt, Germany*

ARTICLE INFO

Article history:
Received 1 August 2008
Received in revised form 3 November 2008
Accepted 3 November 2008
Available online xxx

Keywords:
Field-flow fractionation
Size exclusion chromatography
Copolymer composition
High temperature separation
Diffusion coefficient
Thermal diffusion coefficient

ABSTRACT

Field-flow fractionation (FFF) is a family of analytical techniques developed specifically for separating and characterizing macromolecules, supramolecular assemblies, colloids and particles. It combines the effects of a laminar flow profile with an exponential concentration profile of analyte components caused by their interactions with a physical field applied perpendicular to the flow of a carrier liquid. FFF is undergoing increasingly widespread use as researchers learn of its potential and versatility. This overview underlines the basic principle and theory behind FFF and reviews recent research efforts incorporating flow and thermal FFF methods to characterize natural, biological, and synthetic polymers. These FFF techniques will be discussed in terms of theory and practice. Selected applications of FFF and their coupling capability with other chromatographic techniques or spectrometric detection for the separation and characterization of polymers in organic and aqueous media are presented.

Contents

Abbreviations: AcFFF, acoustic field-flow fractionation; AsFlFFF, asymmetric flow field-flow fractionation; CCD, chemical composition distribution; DEP-FFF, dielectrophoretic field-flow fractionation; dRI, differential refractive index; DLS, dynamic light scattering; ElFFF, electrical field-flow fractionation; FFF, field-flow fractionation; FlFFF, flow field-flow fractionation; FTIR, Fourier transform infrared; GELC, gradient elution liquid chromatography; GrFFF, gravitational field-flow fractionation; HPLC, high performance liquid chromatography; HT AsFlFFF, high temperature asymmetric flow field-flow fractionation; HT SEC, high temperature size exclusion chromatography; HF, hollow fiber; HDC, hydrodynamic chromatography; LCCC, liquid chromatography at critical conditions; LCLC, liquid chromatography near limiting conditions; MgFFF, magnetic field-flow fractionation; MALDI-TOF–MS, matrix assisted laser desorption/ionization time-of-flight mass spectrometry; MT AsFlFFF, medium temperature asymmetric flow field-flow fractionation; MALS, multi-angle light scattering; mAsFlFFF, micro AsFlFFF; MMD, molar mass distribution; MW, molecular weight; MWCO, molecular weight cut-off; NMR, nuclear magnetic resonance; SEC, size exclusion chromatography; SdFFF, sedimentation field-flow fractionation; TEM, transmission electron microscopy; TREF, temperature rising elution fractionation; ThFFF, thermal field-flow fractionation; UV–vis, ultraviolet and visible.

* Corresponding author. Tel.: +27 21 8083172; fax: +27 21 8084967.
** Corresponding author. Tel.: +1 303 273 3245 fax: +1 303 273 3629.
E-mail addresses: rda@sun.ac.za (R.D. Sanderson), krwillia@mines.edu (S.K.R. Williams).

0079-6700/$ – see front matter © 2009 Elsevier Ltd. All rights reserved.
doi:10.1016/j.progpolymsci.2008.11.001

1. Introduction

The synthesis of new polymers with tailored properties is driven by scientific curiosity, practical needs, and profit margins. Intriguing new materials include polymer hybrids that combine biodegradable molecules with oil based monomers, novel architectures that affect rheology, and self-assembled nanoparticle block copolymers in an array of different structures. Ongoing innovations in the synthesis of new polymeric materials are accompanied by a need to extend the limits of existing analytical methods and to develop new analytical techniques with new capabilities. Polymers are polydisperse in their molar mass, chemical composition, functionality, and molecular architecture [1,2], and there is a high demand for information on these distributed properties because of their impact on the performance of the polymer materials. Separation and characterization of heterogeneous polymers (polymers with more that one type of distribution) is highly desired.

A number of different chromatography techniques that exploit different separation mechanisms are commonly used to fractionate polymers. Size exclusion chromatography (SEC) is currently the most commonly used chromatographic technique for polymer separations. In SEC an entropically controlled separation occurs according to hydrodynamic volume or size of molecules [3]. Smaller molecules are retained longer because they are able to diffuse into the pores of the stationary phase, while larger molecules elute first because they are excluded from the pores. While SEC can separate polymers into narrow disperse molecular weight distributions, it is limited by upper molecular weight exclusion limits, sample adsorption to the stationary phase, shear degradation at high pressures and flow rates, and an inability to separate analytes based on composition. In gradient elution liquid chromatography (GELC), separation is based on analyte precipitation and redissolution in a solvent gradient system [4]. Thus gradient elution is dependent on both the molar mass and composition of the polymer. Limitations of GELC include the need to experimentally determine the appropriate eluent conditions from two or more solvents, non-exclusion operating conditions, precipitation of polymer in the packed column, and analyte detection due to a continuously changing mobile phase composition. In liquid chromatography at critical conditions (LCCC), entropic and enthalpic interactions are balanced through the selection of solvent and temperature such that the resulting separation is governed by small differences in the chemistry of the components [5]. It is used for the characterization of copolymers, or functional type distributions, and is highly sensitive to temperature and solvent composition fluctuations which can lead to peak splitting, peak broadening, analyte loss due to adsorption to the stationary phase, and limited reproducibility. Liquid chromatography at limiting conditions (LCLC) belongs to the so-called barrier polymer high performance liquid chromatography (HPLC) approaches. LCLC is less sensitive to mobile phase composition or temperature changes than LCCC. It also has a broader analyte molecular weight operating range, accommodates column overloading, and can handle a wide range of eluent compositions [6]. Separation with temperature rising elution fractionation (TREF) relies on differences in crystallizability and redissolution [7]. Finally, separation by hydrodynamic chromatography (HDC) occurs because analytes of different sizes are excluded differently from regions of low carrier liquid velocity near the surface of the wall. It is a size based separation method and suffers from similar limitations to those of SEC [8].

Two-dimensional (2D) chromatography can be used to obtain information on two different property distributions of a polymer in a single analysis. Orthogonality of the combined separation methods should be as large as possible. Ideally, the coupled techniques should augment or suppress the selectivity of the separation according to one of the molecular characteristics (i.e., molar mass or chemical composition distribution). The technique with the highest separation selectivity for only one feature should be chosen as the first dimension [2,9]. An additional benefit of hyphenated methods that include a separation stage is that the complex sample is spatially separated into more homogeneous components whose properties can be individually measured. This provides a detailed picture of the distribution (size, molecular weight, etc.) and relative amounts of sample components present. Reverse phase followed by normal phase liquid chromatography of polysytyrene-b-polyisoprene copolymers has the ability to resolve analytes that differ by only one styrene or isoprene monomer. Clear oligomeric separation of unique copolymers with specific numbers of each monomer was

Please cite this article in press as: Messaud FA, et al. An overview on field-flow fractionation techniques and their applications in the separation and characterization of polymers. Prog Polym Sci (2009), doi:10.1016/j.progpolymsci.2008.11.001

shown on a 2D plot. Unfortunately, this separation was not extended to molecular weights greater than ~2400 Da [10].

Due to the need for highly detailed information about the molar mass, chemical composition, functionality, and molecular architecture of macromolecular materials, new analytical separation techniques with increased resolution, sensitivity, selectivity and broader applications are constantly sought after. Field-flow fractionation (FFF) is a rapidly emerging technique that meets many of these needs. FFF can fractionate a wide range of analytes including macromolecules, and colloids and particulates suspended in both aqueous and organic solvent carriers [11–14]. FFF can overcome some of the common limitations of traditional chromatographic techniques in several ways:

- Polymers can be simultaneously fractionated based on different physico-chemical characteristics such as size and composition.
- There is no stationary phase, therefore, there are no sample breakthrough effects or sample loss due to adsorption to the stationary phase.
- The upper limit of FFF extends to the 10^9 Da molecular weight range and micron-size particles, thus providing effective separation of microgel components simultaneously with solubilized polymer [15].
- Shear degradation is minimized [11,16–18].
- Materials can be separated with high resolution over a wide size range from 1 nm to 100 μm [12,16].
- Different types of samples can be accommodated because of the physical simplicity and stability of FFF systems and the ease of adjusting experimental conditions.
- The mild operation conditions allow the analysis of fragile analytes such as protein aggregates, supramolecular assemblies, and whole cells [13,19].

Other specific features of FFF techniques were recognized which include the physical simplicity and stability of FFF systems, the minimum sample loss, easy to adjust or change experimental conditions to accommodate different kinds of samples, gentle operation conditions and easy maintenance and field strength programmability. Commercial FFF systems have been available since the late 1980s and are currently available from Postnova Analytics (Landsberg am Lech, Germany), Wyatt Technology Corporation (Santa Barbara, California, USA), and ConSenxus (Ober-Hilbersheim Germany). FFF can also be easily inserted into 2D chromatography setups to provide more detailed information on copolymers [20].

Polymer separation techniques are combined with an appropriate detector(s) for the online or offline determination of various molecular characteristics. The most commonly utilized detectors with FFF are multi-angle light scattering (MALS), differential refractive index (dRI), ultraviolet and visible (UV–vis), differential viscometry, nuclear magnetic resonance (NMR) and Fourier transform infrared (FTIR). MALS, dRI, UV–vis, and viscometry detectors offer the advantage of online detection. Without the separation step, the detection methods listed above provide average values representative of the entire sample population. Matrix assisted laser desorption/ionization time-of-flight mass spectrometry (MALDI-TOF–MS) has also become a workhorse for macromolecular analyses [21–23].

2. Field-flow fractionation

2.1. General principles and modes of operation

Field-flow fractionation was first introduced by J. Calvin Giddings in 1966 [24]. It is an elution based chromatography-like method in which the separation is carried out in a single liquid phase. FFF is characterized by the use of an external field applied perpendicularly to the direction of sample flow through an empty, thin ribbon-like channel (Fig. 1a). Due to the high aspect ratio of the FFF channel a laminar parabolic flow profile develops, with

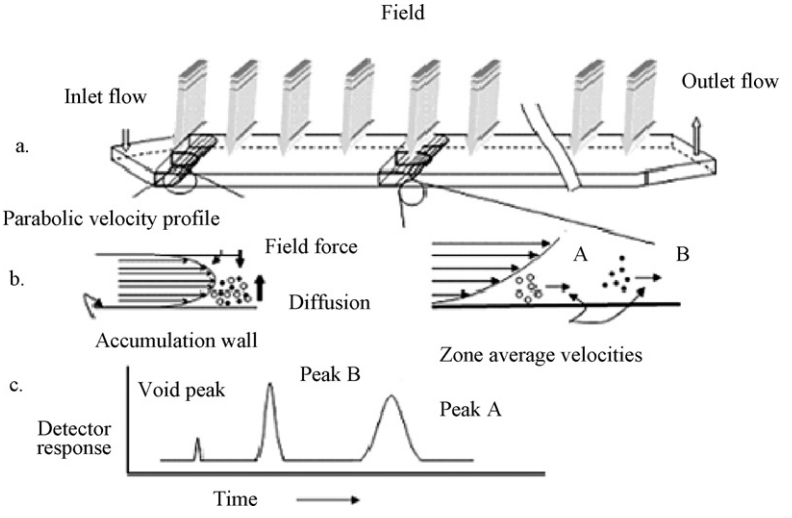

Fig. 1. (a) Schematic representation of an FFF channel cut-out, (b) exploded views of the normal mode separation mechanism of two components A and B (faster diffusing B components are located at higher elevation in faster flow velocity streamlines and are thus eluted earlier than slower diffusing A components) and (c) a typical FFF fractogram.

Please cite this article in press as: Messaud FA, et al. An overview on field-flow fractionation techniques and their applications in the separation and characterization of polymers. Prog Polym Sci (2009), doi:10.1016/j.progpolymsci.2008.11.001

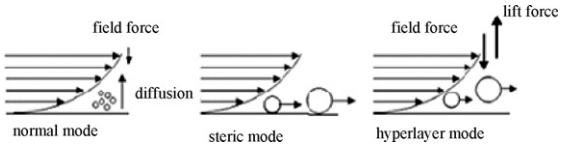

Fig. 2. Schematic representation of different modes of operation that can occur in FFF.

flow velocity increasing from near zero at the channel walls to a maximum at the centre of the channel (Fig. 1b). The perpendicularly applied force drives the sample toward the accumulation wall. A counteracting diffusive force develops due to the concentration build up at the wall and drives the analyte back towards the centre of the channel. When the forces balance, steady state equilibrium is reached and an exponential analyte concentration profile is built up. Retention occurs when analytes reside in flow velocity zones slower than the average flow velocity of the carrier liquid passing through the channel. Separation occurs because different analytes reside in different flow velocity zones.

The normal mode of separation, in which diffusion plays an important role in controlling component distribution across the channel, is the most widely used mechanism [12,16]. A schematic illustration of the basic principle of normal mode FFF separation and a typical resulting fractogram are shown in Fig. 1. The fractogram is a detector response versus elution time (or elution volume) curve.

Analytes can be separated by different mechanisms (modes of operation) in FFF that arise from different opposing forces The mode of operation determines the elution order of analytes, along with other separation characteristics such as selectivity and resolution. Three widely used modes that can be implemented in any FFF technique are normal, steric, and hyperlayer [11,16,25] and are shown in Fig. 2. The normal mode (based on Brownian motion of the analyte in the channel) is usually used for analyte sizes smaller than ~1 μm. Smaller component populations accumulate in regions of faster streams of the parabolic velocity profile and elute earlier than larger components. Steric mode is applicable for components larger than ~1 μm where diffusion becomes negligible and retention is governed by the distance of closest approach to the accumulation wall. Small particles can approach the accumulation wall more closely than large particles and thus the former's centre of mass is in the slower flowing streamlines. The elution order in steric mode is from largest to smallest. Finally, lift or hyperlayer mode is one in which lift forces drive sample components to higher velocity streams located more than one particle radius from the accumulation wall. These hydrodynamic lift forces occur when high flow velocities are used. The elution order is the same as in the steric mode. Most polymers are separated by the normal mode mechanism because their dimensions are less than 1 μm [12,16].

The terminology used to describe different modes of operation is historically based and follows the development of FFF. The "normal" mode was the first observed mode of operation [16]. The term "steric" evolved later to describe a second separation mechanism observed when FFF was extended to >1 μm particles [26]. As the flow rate was increased to shorten the analysis time, it was observed that the micron-sized particles eluted significantly earlier than predicted by the steric mode retention time equation. It became evident that these particles' centers of mass were located in flow streams well above one particle radius from the FFF accumulation wall [27]. This led to the introduction of the term "hyperlayer" to describe the formation of analyte layers above the channel wall as a result of two opposing forces [28]. While steric mode separations are experimentally achievable, most separations involving micron-sized analytes are usually, partially if not entirely, in the hyperlayer mode.

2.2. Fields and channel geometries in FFF

Various fields have been used in FFF depending on the nature of the material to be analyzed. The criteria for an effective field are sufficient strength and selectivity to achieve separation, and ease of implementation. Each type of field interacts with a different physicochemical property of the analyte [12,16]. Typical fields include a cross-flow stream, temperature gradient, electrical potential, centrifugal force, gravitational force, dielectrophoretic, standing acoustic wave and magnetic fields. These give rise to several FFF techniques including flow (FlFFF), thermal (ThFFF), electrical (ElFFF), sedimentation (SdFFF), gravitational (GrFFF), dielectrophoretic (DEP-FFF), acoustic (AcFFF) and magnetic (MgFFF) field-flow fractionation. Analyte retention and separation in these different FFF techniques are achieved according to different analyte properties such as size, thermal diffusion, charge, density, mass, and magnetic susceptibility [11,12,16,25,29–31]. Of these techniques, FlFFF, ThFFF, and SdFFF are commercially available with the first two being the workhorses for polymer separation and analysis.

Field strength is the most important experimental condition in FFF because it has a strong effect on the resolution and separation time. With field programming, the field strength is changed according to a decay function over the course of the analysis. Field programming is useful when studying broad distributions of molar masses or particles [11,25,32,33]. It is used to optimize resolution and analysis time, and enhance the detectability of fractionated analytes. Several types of field programming have been used including linear, parabolic, exponential, and step-wise decay functions [11,16,25,32–35]. Field programming in FlFFF and ThFFF is implemented by reducing the cross-flow rates and temperature gradients, respectively. Generally, for lower mass and smaller particles higher field strength is required.

The FFF channel is constructed by clamping a thin spacer (usually of Mylar or polyimide) with the desired geometric cut-out between two blocks with flat surfaces. The block material must be compatible with the carrier liquid and transmit the applied field. The ribbon-like channel in Fig. 1a is the most commonly employed channel geometry. With this ribbon-like structure a perpendicular orientation of most fields can be achieved. Because diffusion is a slow process, the channel thickness (w) must be small enough that the sample reaches equilibrium in a reasonable short time. The length of the channel (L) needs to

Please cite this article in press as: Messaud FA, et al. An overview on field-flow fractionation techniques and their applications in the separation and characterization of polymers. Prog Polym Sci (2009), doi:10.1016/j.progpolymsci.2008.11.001

be long enough to allow adequate retention time differences between the analytes. Typical channel dimensions are thicknesses of 50–500 μm, breadth of 2 cm, and tip-to-tip lengths of 25–90 cm. Triangular end pieces are used to allow smooth inlet and outlet flow. Due to the high aspect ratio (breadth to thickness) of ~100, this type of rectangular channel can be considered as two infinite parallel plates in between which the parabolic laminar flow velocity can easily develop and edge flow perturbation is minimized. Trapezoidal shaped channels (inlet breadth is greater than outlet breadth) as proposed by Litzen and Wahlund are used in AsFlFFF to allow more constant cross-flow along the length of the channel [36,37]. For the rectangular channel, the breadth (b) is constant and the total area of the accumulation wall (A_{ac}) is equal to bL, where the effective length (L) is equal to ($L_{tt} - L_1$). The L_{tt} is tip-to-tip channel length and L_1 is equal to L_2. For the trapezoidal channel, the breadth is a function of distance (z) and (A_{ac}) is equal to $\{[b_o (L_{tt} - L_2) + b_L (L_{tt} - L_1)]\}/2$.

An exponentially decreasing channel breadth was designed by Williams [38] to provide constant volumetric flow rates along the length of the asymmetric channel. Another channel arrangement of a cylindrical shape utilizing hollow fiber (HF) membranes has been also employed in FFF [39,40]. A radial cross-flow is applied to drive the components to the fiber wall. An in-depth discussion of channel construction for various FFF techniques can be found in reference [16]. A brief description of channel components and construction will be given in each respective FFF section.

Channel miniaturization is a current research topic in both FlFFF and ThFFF, and has been discussed in a number of recent reports [41–50]. The benefits of reducing the channel dimensions include decreased sample size, carrier liquid consumption and analyte retention time and improved resolution, portability, and disposability. Miniaturized AsFlFFF channels have been constructed with typical dimensions of 250–500 μm (thickness) × 90–110 mm (length) with channel a breadth of 7 mm at the sample inlet that tapers to 3 mm at the channel outlet. Micro AsFlFFF (mAsFlFFF) has been utilized to successfully separate protein mixtures ranging in MW from 29–669 kDa and protein dimers from monomers. Two unique applications of mAsFlFFF include sizing of high density, low density, and very low density lipoproteins and differentiation of single strand DNA containing 50 and 100 bases. Single strand DNA bound and unbound to replication protein A showed slightly different retention times suggesting that mAsFlFFF could be used to investigate DNA-protein binding activity [41,43]. Miniaturized ThFFF channels with dimensions of the order of 25–250 μm (thickness) × 1–10 mm (breadth) × 50–100 mm (length) have been built and tested. Most of the reported applications have focused on separations of particles (polystyrene, silica, bacteria) ranging in size from ~60 nm to several micrometers using an aqueous based carrier liquid. The separation of a mixture of 115, 1030, and 10,000 kDa polystyrene standards was accomplished using tetrahydrofuran as the carrier liquid. These results demonstrated the range of MW and particle size that can be analyzed by the micro thermal FFF channel [44–50].

2.3. Theoretical background

2.3.1. Analyte retention

The theory and development of FFF techniques have been described in detail in many publications [11,12,16,24,36,51]. Hence, it will be described only briefly here.

A general description of retention and separation mechanisms was given in Section 2.1. The parabolic flow velocity profile ($\upsilon(x)$) across the channel depicted in Figs. 1 and 2 can be described by Eq. (1):

$$\upsilon(x) = 6\langle\upsilon\rangle \left[\left(\frac{x}{w}\right) - \left(\frac{x}{w}\right)^2 \right] \quad (1)$$

where $\langle\upsilon\rangle$ denotes the average velocity of the carrier liquid across a channel of thickness w and x is the distance from the accumulation wall ($x = 0$ at the accumulation wall). Eq. (1) can be derived by integration of the Navier–Stokes equation for fluid flow (with constant viscosity) between two parallel plates.

The analyte's concentration profile ($c(x)$) is determined by the field-induced transport of analyte towards the wall and the diffusion away from the wall to lower concentration regions. When these two opposing transport processes are in equilibrium there is no net flux of material and the concentration profile has an exponential distribution as described by Eq. (2):

$$c(x) = c_o e^{\left(-\frac{U}{D}\right)x} \quad (2)$$

where c_o is the analyte concentration at the accumulation wall ($x = 0$), D is the ordinary diffusion coefficient and U is the particle velocity induced by the field force (it is the transverse velocity of the analyte toward the accumulation wall).

Diffusion of a Brownian particle depends on the friction factor (f) and can be expressed by the Nernst–Einstein equation: $D = kT/f$, where k is the Boltzmann's constant and T is the absolute temperature. Friction force for a particle moving with velocity (U) in a host medium is related to the field force (F) as: $F = fU$, then the diffusion coefficient becomes: $D = [kT(U/F)]$. A mean layer thickness (l) of the sample cloud is defined as the distance from the accumulation to the centre of mass of sample zone. It is expressed as the ratio of thermal energy to the applied force: $l = kT/F = D/U$.

A dimensionless zone thickness (λ), known also as the retention parameter, is defined as the ratio (l/w). It represents the degree of zone compactness relative to the channel thickness as well as of the volume fraction of sample layer. It is a measure of the extent of interaction between the field force and the sample components. For general FFF systems, λ can be expressed as:

$$\lambda = \frac{kT}{wF} = \frac{D}{Uw} \quad (3)$$

Thus, the concentration profile expression in Eq. (2) can be also written in other forms such as:

$$c(x) = c_o e^{\left(-\frac{x}{l}\right)} = c_o e^{\left(-\frac{x}{\lambda w}\right)} \quad (4)$$

It can be seen from Eq. (4) that the analyte concentration decreases exponentially as the distance from the accumu-

lation wall increases. Therefore, with sufficient interaction with the applied external field, the majority of the analyte will reside within a few micrometers of the accumulation wall surface. It is assumed that the interactions between the particles and the wall and between the particles themselves are insignificant.

The retention parameter (λ) is directly related to physiochemical parameters of the retained components and links theory to experiment as will be discussed in the following sections. Different terms are substituted for F depending on the type of field that is employed. The expression for λ shown in Eq. (3) takes on different forms specific to the type of field used and reflects the field's characteristic interactions with different physicochemical properties of the analyte.

Retention refers to the retarding of analyte zones through their confinement to flow streamlines with velocities less than the average velocity of the carrier liquid. This can be described by a retention ratio (R) defined as the ratio of the average velocity of the analyte zone (υ_{zone}) to the average velocity of the carrier liquid $\langle\upsilon\rangle$. R can be calculated from the concentration and carrier liquid flow velocity profiles by Eq. (5):

$$R = \frac{\upsilon_{zone}}{\langle\upsilon\rangle} = \frac{\langle c(x)\upsilon(x)\rangle}{\langle c(x)\rangle\langle\upsilon(x)\rangle} \tag{5}$$

where $\upsilon(x)$ and $c(x)$ are the parabolic velocity profile and concentration profile respectively seen in Eqs. (1) and (2). The brackets denote average values. Substituting Eqs. (1) and (2) into Eq. (5), an expression relating λ and R can be derived:

$$R = 6\lambda\left[\coth\left(\frac{1}{2\lambda} - 2\lambda\right)\right] \tag{6}$$

R can also be determined empirically from the ratio of the measured void time t^0 to the retention time t_r. Under non-overloading conditions, retention times measured at peak maxima are excellent approximations if the elution profiles are Gaussian distributions [16]. For λ values less than 0.02, R can be calculated with an error of ~5% using the 6λ approximation:

$$R = \frac{t^0}{t_r} = \frac{V^0}{V_r} \approx 6\lambda \tag{7}$$

where V^0 is the volume of the FFF channel and V_r is the retention volume. Values of λ obtained from experimentally measured retention times can also be used to calculate various physiochemical parameters of the analyte. The retention parameter λ is the link between theoretical and measurable experimental parameters through the retention ratio (R) or the retention time t_r.

The theoretical development of the FFF retention was based on a number of assumptions which include the parabolic flow profile between infinite parallel plates, the absence of analyte–analyte and analyte–FFF wall interactions, and uniformity of the applied field.

As mentioned earlier, most polymers are separated by the normal mode in which the smaller molecules elute first. This is the opposite of SEC in which the larger molecules elute first.

2.3.2. Efficiency and resolution

Due to the assumption of an exponential concentration profile of the analyte and of the parabolic flow profile used in the theoretical development of FFF retention theory, significant errors in retention parameters may arise under certain conditions [16]. FFF measurements also involves deviations between the experimental results and the expected theoretical behavior due to various effects including zone broadening, overloading, solvent effects, analyte–wall interactions, analyte–analyte interactions, and non-uniformity of field strength. Some of these effects, e.g., zone broadening, are unavoidable and can only be corrected empirically. Many effects can be minimized by precise control and measurements of the different parameters such as flow rates, concentration and temperature. These deviations may be accounted for by using on-line detectors, e.g., light scattering, that provide independent measurements of size and/or molecular weight.

Efficiency and resolution analysis allow various techniques to be compared and are utilized for the optimization of experimental variables and estimation of component properties. As with chromatography, the separation efficiency of FFF techniques can be described by the theoretical plate height (H). It is a measure of dispersion (or zone broadening) and is reflected in the width of a sample peak. Main factors affecting zone spreading are non-equilibrium (H_n), axial diffusion (H_d), sample polydispersity (H_p) and instrumentation and operational effects (H_i). These factors contribute to the plate height in an additive form ($H = H_n + H_p + H_d + H_i$).

The non-equilibrium term, H_n, is the main contributor to the measured peak width. This effect is due to the differential axial movement of the zone components because they are located in different velocity streamlines across the channel thickness. H_n is largely dependent on the flow rate and the channel dimensions. It has been shown that H_n is a complex function of the retention parameter λ as in Eq. (8) [16]:

$$H_n = \chi(\lambda)\frac{w^2\langle\upsilon\rangle}{D} = \frac{24\lambda^3 w^2\langle\upsilon\rangle}{D} \tag{8}$$

where the function $\chi(\lambda)$ becomes equal to $24\lambda^3$ as λ approaches zero.

Axial diffusion (H_d) describes the effect of longitudinal diffusion due to axial concentration gradients. H_d is significant only when very low flow velocity is used. In the case of high molecular weights, diffusion coefficients are small and the contribution of H_d to the plate height is often negligible. For highly polydisperse samples the polydispersity contribution H_p to the plate height can be significant. The H_i represents the effects of relaxation, triangular ends, injection of finite sample volume and detection. In a well-designed system the effect of H_i can be reduced to a negligible level.

Assuming a Gaussian shaped peak the plate height can be obtained from the number of theoretical plates N and peak standard deviation σ from the following expressions:

$$N = \frac{L}{H} = \left(\frac{L}{\sigma}\right)^2 \tag{9}$$

Please cite this article in press as: Messaud FA, et al. An overview on field-flow fractionation techniques and their applications in the separation and characterization of polymers. Prog Polym Sci (2009), doi:10.1016/j.progpolymsci.2008.11.001

Using H and N allows comparison between various instruments with lower H or higher N preferred.

The resolution or fractionation power is referred to the separation ability of a system. It is simply the degree of the overlap of two peaks and can be described mathematically by the resolution index (R_s) given as:

$$R_s = \frac{\Delta t_r}{4\sigma_r} = \frac{\Delta V_r}{4\sigma_v} \quad (10)$$

where Δt_r and ΔV_r are the retention time and the retention volume differences and σ_r and σ_v are the average standard deviations of the two zones (in time and volume units, respectively). Peaks are completely overlapped if R_s is equal to zero and continue to separate as R_s increases. The resolution index is a function of the channel length, the plate height, the relative molecular mass differences and the selectivity.

The uniqueness of FFF methods is their capability for high resolution separation of components. A comparison of polymer resolution in ThFFF and SEC has been made by Gunderson and Giddings [52]. The measured resolution for three different binary polymer mixtures was found to be higher for ThFFF than that for SEC. Calculated resolution values with the polydispersity corrections showed that ThFFF had a significant advantage over SEC.

3. Flow and thermal field-flow fractionation

3.1. Symmetric and asymmetric flow field-flow fractionation

Two types of flow FFF are considered in this review: symmetric flow field-flow fractionation (FlFFF) and asymmetrical flow field-flow fractionation (AsFlFFF). Symmetric FlFFF was introduced in 1976 by Giddings [51]. In this first form of flow FFF, the channel spacer is clamped between two parallel plastic blocks fitted with porous ceramic frits (2–5 μm pores) in each wall [16]. A cross-flow is applied as the 'field' perpendicular to the channel flow. Cross-flow enters the channel through the porous frit on the top wall and exits the channel through an ultrafiltration membrane, overlaying a second porous frit at the bottom wall (the accumulation wall).

Ultrafiltration membranes are classified by their molecular weight cut-off (MWCO) values: membranes with lower nominal values prevent smaller analytes from permeating the membrane. Various types of membranes: regenerated cellulose, polyimide/poly(ethyleneterephthalate), sulfonated polystyrene, polypropylene, polyethersulfone, polyacrylamide, and polyacrylonitrile have been used in FlFFF [16]. When selecting a membrane, membrane thickness, smoothness, chemical and mechanical stability, as well as the solute size/molecular weight and interactions between solute and membrane, should be carefully considered.

The asymmetrical version, AsFlFFF, was first introduced in 1987 [48]. A membrane is also used here as the accumulation wall. However, AsFlFFF differs from FlFFF in that the channel has only a single permeable wall (the accumulation wall). The upper porous wall is replaced by a solid wall that is impermeable to the carrier liquid. A single channel inlet flow is split into the channel flow and the cross-flow. The ratio between the two depends on operator controlled in-line flow resistances. AsFlFFF has the following advantages over FlFFF: simpler construction and the ability to visualize the sample through a transparent upper wall [36]. A schematic representation comparing FlFFF and AsFlFFF is shown in Fig. 3.

As mentioned previously, λ is unique for each type of FFF 'field' and interacts to different extents with different analytes physicochemical properties. In both FlFFF and AsFlFFF a cross-flow is applied as the external field and the analyte components are driven to the accumulation wall with a velocity U (equal to $\dot{V}_c/A_{ac}$). The surface area of the accumulation wall A_{ac} is equal to the volume of the channel (V^0) divided by the channel thickness. Using Eq. (3), λ can be described by Eq. (11):

$$\lambda = \frac{DV^0}{\dot{V}_c w^2} \quad (11)$$

where $\dot{V}_c$ the cross-flow volumetric flow rate and D is the diffusion coefficient of the analyte.

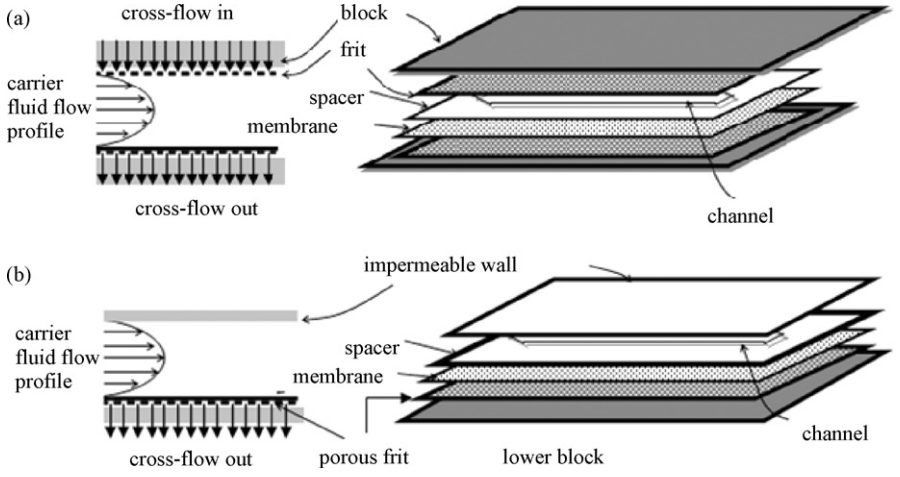

Fig. 3. A schematic representation of (a) symmetric (FlFFF) and (b) asymmetric (AsFlFFF) channel structures.

Please cite this article in press as: Messaud FA, et al. An overview on field-flow fractionation techniques and their applications in the separation and characterization of polymers. Prog Polym Sci (2009), doi:10.1016/j.progpolymsci.2008.11.001

For symmetric FlFFF, substitution of Eq. (7) into Eq. (11) and rearrangement yields the analyte retention in terms of D in Eq. (12):

$$t_r = \frac{t^0}{6\lambda} = \frac{t^0 w^2 \dot{V}_c}{6DV^0} = \frac{w^2 \dot{V}_c}{6D\dot{V}} \quad (12)$$

where $\dot{V}$ the volumetric flow rate along the channel: $\dot{V} = V^0/t^0$. Using the Stokes–Einstein equation: $D = kT/3\pi\eta d_h$ where η is the dynamic viscosity of the carrier fluid, the hydrodynamic diameter (d_h) can be directly calculated from retention data using Eq. (13):

$$d_h = \frac{2kTV^0}{\pi\eta\dot{V}_c w^2 t^0} t_r \quad (13)$$

In AsFlFFF, λ is also represented by Eq. (7) because the applied force field is a cross-flow. However, because the channel inlet flow is split into the channel flow and the cross-flow, the analyte retention time equation is different to that for symmetric FlFFF. The retention time t_r can be approximately calculated from Eq. (14) and accounts for the lack of cross-flow at the upper nonporous wall [36]. Again, substitution of the Stokes–Einstein equation for D will yield the d_h in terms of t_r:

$$t_r = \frac{w^2}{6D} \ln\left(1 + \frac{\dot{V}_c}{\dot{V}_{out}}\right) \quad (14)$$

Sample relaxation and focusing are used in AsFlFFF whereas only the former is used in FlFFF. These procedures serve to improve resolution and decrease peak widths. Interestingly, AsFlFFF has been shown to produce smaller plate heights, i.e., narrower bands, than FlFFF. Frit inlet and frit outlet FlFFF and AsFlFFF have also been used to reduce relaxation and analysis times, minimize sample interaction with the membrane, and concentrate the separated sample on-line [53]. The latter is an important feature when working with a detector, e.g., MALS, that requires higher sample concentrations.

3.2. High temperature asymmetric flow field-flow fractionation

Elevation of temperature can enhance the separation and analysis time in FFF [16,54]. The elevated temperature improves the solubility of many polymers and results in rapid diffusion transport. A decrease in band broadening can be also gained.

Medium temperature asymmetrical flow field-flow (MT AsF1FFF) and (HT AsF1FFF) fractionation systems have been developed and distributed by Postnova Analytics (Landsberg am Lech, Germany). HT AsF1FFF has been specifically developed for the separation and characterization of high molecular mass polyolefin resins. Different detectors such as infrared (IR), refractive index (RI), MALS and viscometry were applied. In HT AsFlFFF, a stainless steel channel and a flexible ceramic accumulation wall membrane is used. This allows measurements with chlorinated organic solvents like 1,2,4-trichlorobenzene (TCB) at temperatures up to 220 °C. The trapezoid channel is cut from a Mylar spacer with a thickness of 250–350 μm. The channel-length is 27.8 cm with a maximum width of 2 cm. A ceramic foil with a pore size of approximately 10 nm was used as membrane. To enhance the performance of the polymer separation a special focusing flow was implemented. This focusing flow is a second input flow, which enters the channel close to the middle and divides itself into two sub streams, as is shown in Fig. 4. One part of the flow meets the injection flow near the beginning of the channel. Together the two flows form a sharp barrier and leave the channel through the membrane as cross-flow. In the region were both flows come into contact with each other, the sample transported by the injection flow is focused laterally and will rest at the same position until the focus flow stops. The second focus flow substream leaves the channel through the outlet and provides a constant detector flow during the focusing step. This new technique allows the polymer molecules to be retained at the beginning of the channel after the injection. As a result the molecules can be separated with minimal longitudinal diffusion, which results in less band broadening.

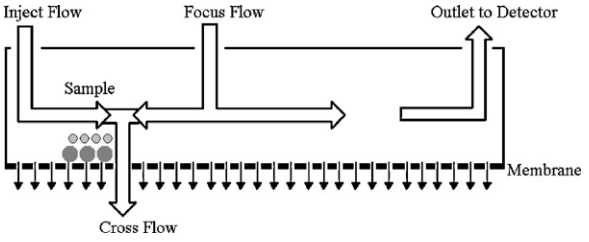

Fig. 4. Flow scheme of the AsFlFFF focussing step.

HT AsFlFFF is generally a complementary technique to high temperature size exclusion chromatography (HT SEC). It is reported that the selectivity and the efficiency of the FFF separation are superior for high molecular weight species. However, SEC performs better in the separation of lower molecular weight material [55]. Due to the low molecular weight cut-off limit of the ceramic membrane, low molar mass polymers cannot be fractionated by HT AsFlFFF. Presently, the size of the pores in the membrane causes a polyethylene low molecular weight cut-off of approximately 5×10^4 g/mol [56], leading to a very low recovery for polydisperse samples with a high amount of small molecules. New membrane architectures and materials need to be developed to solve this problem. The slot outlet technology should be realized for HT AsFlFFF in the near future. During elution the sample moves close to the accumulation membrane. The thickness of the sample layer is typically 1–10 μm. The remainder of the channel contains only pure solvent. In passing through the detector, the sample layer and the solvent layer are mixed together leading to lower concentration. Using the slot outlet technology, the solvent layer can be removed by a separate pump. The remaining solute layer then passes through the detector and the peak heights are thus amplified. The signal-to-noise ratio has been shown to improve 5–8 times for a polymer separation using low temperature AsFlFFF [57]. In future, the HT AsFlFFF should be a universal and suitable tool next to HT SEC, because there are no restrictions such as shear degradation or limited separation of ultra high molecular weight analytes. Presently, the problem of losing small molecules is resolved partly for linear polyolefins by combining HT SEC and HT AsFlFFF measurements [55].

Please cite this article in press as: Messaud FA, et al. An overview on field-flow fractionation techniques and their applications in the separation and characterization of polymers. Prog Polym Sci (2009), doi:10.1016/j.progpolymsci.2008.11.001

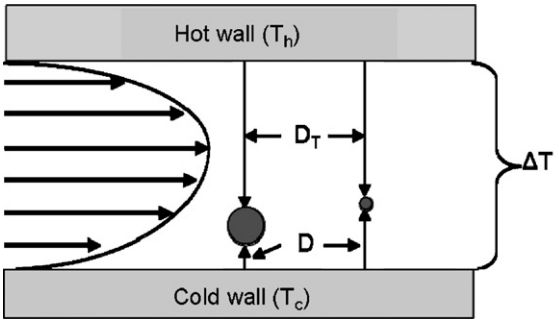

Fig. 5. A schematic illustration of the ThFFF channel and separation. The hot and cold wall temperatures are denoted as T_h and T_c, respectively.

3.3. Thermal field-flow fractionation

ThFFF is one of the most useful FFF techniques for polymer analysis and has been proven to be suitable for the molecular weight analysis of various synthetic polymers in organic solvents. The main advantages of ThFFF over SEC are its sensitivity to both molecular mass and chemical composition and its higher resolution and selectivity for polymers with molecular weights greater than 100 kDa [52].

Thermal FFF systems are produce by Postnova Analytics (Landsberg am Lech, Germany). The ThFFF channel is constructed by clamping a spacer with a geometric cut-out between two metal blocks. The metal blocks are made of copper and have mirror finished plating applied to the surface. The plating must be inert to a wide variety of solvents. Chlorinated solvents should be avoided as carrier liquids because they will etch common nickel or chromium plating. A temperature gradient is applied perpendicularly to the axial carrier liquid flow. To achieve the temperature gradient, the hot wall is kept at an elevated temperature (T_h) through the use of software controlled heating rods and the cold wall is kept cool at lower temperature (T_c) using a recirculating chiller. A temperature drop (ΔT) equal to T_h minus T_c is usually in the range 30–100 K, which results in a strong temperature gradient (up to 10^4 K/cm in a 100 μm thickness channel). ThFFF channels are usually pressurized to 8–10 bars to increase the boiling point of the carrier liquid. Analytes are driven to the cold wall (accumulation wall) by their interaction with the applied temperature gradient. This mass transport is termed thermal diffusion, and is represented by the thermal diffusion coefficient (D_T). A schematic illustration of a cross sectional view of the ThFFF channel is presented in Fig. 5.

Assuming the applied temperature gradient is linear across the channel thickness λ can be represented by Eq. (15):

$$\lambda = \frac{D}{D_T \Delta T} \tag{15}$$

where D is the ordinary diffusion coefficient. D_T is affected by the chemical composition of polymers and the carrier liquid and is independent of the molar mass of many homopolymers [16]. As a consequence, ThFFF can be used to fractionate polymers and copolymers according to chemical composition.

In ThFFF, R can be measured experimentally and related to λ. However, a modified form of Eq. (5) must be used to account for the deviation from the parabolic velocity flow profile that arises from changes in carrier liquid viscosity and thermal conductivity across the channel thickness due to the applied ΔT. (The velocity profile is skewed upwards, with the maximum velocity located above the midplane of the channel [58].) The modified equation includes a velocity distortion factor term (ν) as shown in Eq. (16) [59].

$$R = 6\lambda[\nu + (1 - 6\lambda\nu)\left[\coth\frac{1}{2\lambda} - 2\lambda\right] \tag{16}$$

When ν is equal to zero, the parabolic profile is regained. Values for ν can be found in reference [58]. The use of binary solvents can have a pronounced effect on the velocity profile shape and the retention levels. For example, a binary solvent mixture can enhance polymer retention if the better solvent for the polymer is partitioned towards the cold wall when under the influence of the thermal gradient [58]. The opposite effect can also be observed. As with FlFFF, field programming can be employed in ThFFF by varying the applied thermal field ΔT during the separation process. The same types of programming used in FlFFF can be applied to ThFFF, but the most commonly applied programming is a power decay function for $\mathbf{\Delta} T$.

ThFFF is an absolute molecular mass characterization method only if the Soret coefficient (D_T/D) is known, otherwise a system calibration is required [60–62]. Calibration of the ThFFF channel can be accomplished using narrow polymer standards to establish the relationship between the molar mass of polymers and retention volume. A calibration curve is constructed by plotting $\log D/D_T$ versus $\log M$, or $\log M$ versus log retention time where M is an average molecular weight. The ratio D/D_T is calculated from the measured retention times for each standard using Eqs. (11) and (12) [16,60–62].

4. FFF applications to polymer analysis

While this review focuses on the application of FFF for the separation and analysis of polymers it should be noted that FFF can be used to characterize a broad range of analytes including proteins [39,40,63,64], polysaccharides [35,65–73], synthetic macromolecules [74–80], microgels [15,80], nanoparticle suspensions [81–85], environmental pollutants [86], humic and fulvic substances [87,88], and chemical mechanical polishing slurries [89]. It can also be used to quantitatively determine analyte adsorption to membrane and nanoparticle surfaces [90,91].

FlFFF and ThFFF are the most commonly used FFF techniques for polymer analysis. These techniques can be used for the determination of molar mass or particle mass and their distributions, hydrodynamic radius or particle diameter, diffusion coefficient, thermal diffusion coefficient, Soret coefficient, physiochemical and surface properties and sample polydispersity.

Please cite this article in press as: Messaud FA, et al. An overview on field-flow fractionation techniques and their applications in the separation and characterization of polymers. Prog Polym Sci (2009), doi:10.1016/j.progpolymsci.2008.11.001

4.1. The universality of flow field-flow fractionation and its applicability to polymer analysis

Flow field-flow fractionation (symmetric and asymmetric) is considered the most universal FFF technique because all analytes will be transported by a flowing stream. It is applicable to a wide size range, with the lower limit determined by the molecular weight cut-off of the membrane and the upper limit determined by the channel thickness. Coupling FlFFF or AsFlFFF with light scattering and concentration detectors such as dRI and UV–vis provides powerful methods to fractionate and characterize polymers and eliminates the need for standards. The FFF separation, on the other hand, produces the monodisperse samples essential to MALS. Until recently, FlFFF and AsFlFFF applications were limited to aqueous systems. However, organic compatible channels (ambient and high temperature) with suitable membranes have recently been introduced and successfully applied to polyethylene homopolymers and styrene–butadiene rubber [56,92].

FlFFF has been successfully used to fractionate mixtures of sulfonated polystyrene standards with molecular weights ranging from 18–3000 kDa [93]. Linear cross-flow field programming was used and shown to improve the separation efficiency for the high molar mass and broadly dispersed polymer samples.

FlFFF was used to characterize core-shell particles with cores made from 20/80 weight percent styrene/butyl methyl acrylate and shells composed of various acrylic acids with either carboxylated or hydroxlated end groups. The swelling behavior of the particles was measured as a function of pH and ionic strength of the carrier liquid. By measuring differences in particle retention times it was determined that the carboxlyated shells showed greater swelling than the hydroxylate shells [81]. Additionally, the swelling was found to be a function of only the shell as the cores did not show changes in retention times under different carrier liquid conditions.

Hydrophobically modified pullulans in aqueous solutions have been studied by FlFFF–MALS and SEC [67]. Better results and more information were obtained by FlFFF as it did not suffer the interactions between the hydrophobic segments and the stationary phase as observed in SEC.

Frit inlet AsFlFFF was used to fractionate five different sizes of polystyrene latex bead standards (0.050, 0.135, 0.222, 0.300, and 0.426 μm) with different ratios of sample injection flow rate to frit inlet flow rate as shown in Fig. 6 [94]. This figure demonstrates the capability of flow FFF techniques to quickly fractionate analytes with high resolution across a broad size range. Water soluble poly(*N*-isopropylacrylamide) was studied by AsFlFFF, SEC and DLS [95]. Results obtained using the three methods were in good agreement with the exception of the high molar masses, where the average molar mass obtained by SEC was lower than that obtained by AsFlFFF. This may be due to shear degradation of the polymer in the SEC column.

The analysis of various polysaccharides including starch, cellulose, pullulan, sodium hyaluronate, and gelatine nanoparticles have been accomplished by FlFFF or AsFlFFF. Weight average molecular mass and radius of gyration R_g of cationic potato amylopectin starch derivatives were found

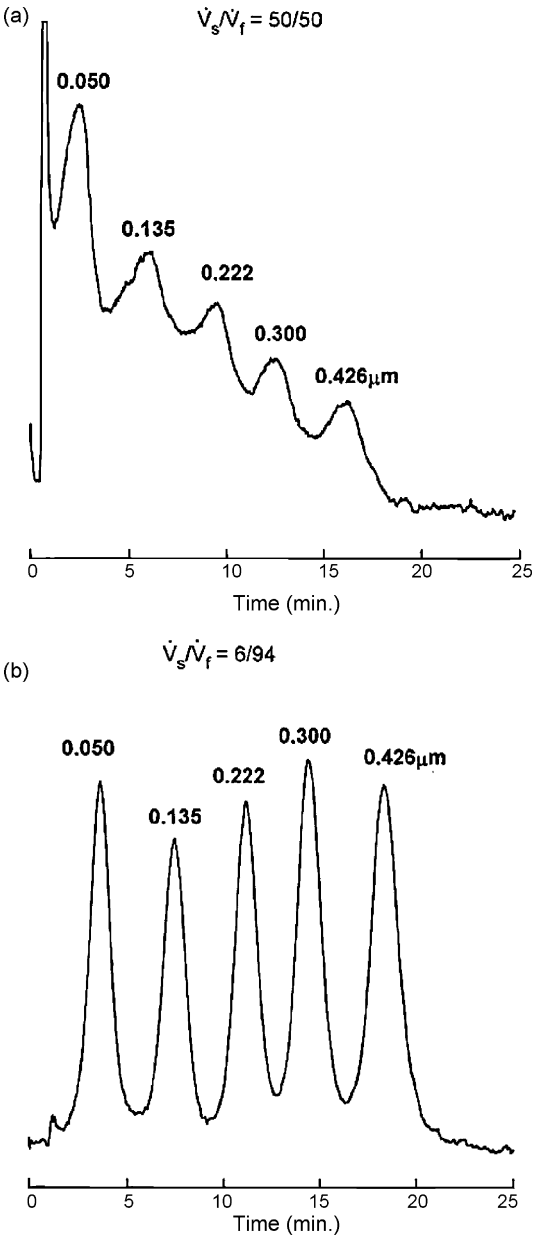

Fig. 6. Separation of 0.050, 0.135, 0.222, 0.300, 0.426 μm polystyrene latex standards by stopless flow injection in a frit inlet asymmetrical-FlFFF obtained at two different ratios of sample injection flow rate to frit inlet flow rate: (a) 50/50 and (b) 6/94. Reprinted from ref. [94] with permission from ACS.

to be 5.2×10^7 g/mol and 340 nm, respectively [70]. It was also observed that charge interactions with the membrane increased with the cross-flow rate and the sample concentration. This can lead to sample loss on the membrane surface and irreproducibility of the fractionation. Charge interactions between the membrane and analyte are not uncommon in FlFFF and can be overcome by adding a surfactant to the carrier liquid or adjusting the ionic strength of the carrier liquid to shield the respective charges. AsFlFFF coupled with MALS and dRI has been employed for the analysis of amylopectins with molar masses in the range of

Please cite this article in press as: Messaud FA, et al. An overview on field-flow fractionation techniques and their applications in the separation and characterization of polymers. Prog Polym Sci (2009), doi:10.1016/j.progpolymsci.2008.11.001

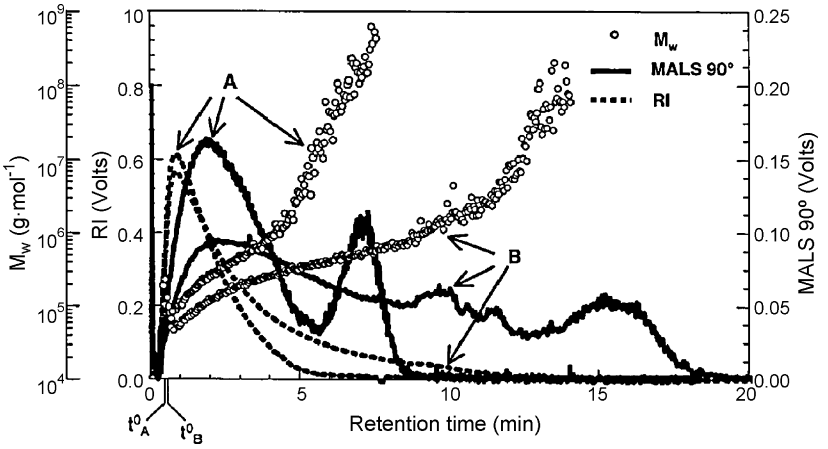

Fig. 7. Weight-average molar mass of ethylhydroxyethyl cellulose obtained at two different cross-flow rates ((A) 0.21 and (B) 0.42 mL/min) using AsFlFFF coupled with MALS and RI. Reprinted from ref. [69] with permission from ACS.

10^7–10^9 g/mol [71]. Flow rates and steric/hyperlayer effects were observed due to the large hydrodynamic radius of the amylopectin macromolecules.

AsFlFFF connected to MALS and RI detectors (AsFlFFF–MALS/dRI) has been utilized to determine the molar mass distribution and molecular radius of ethylhydroxyethyl cellulose at different cross-flow rates [69]. Results presented in Fig. 7 show the potential of the AsFlFFF–MALS combination to fractionate and characterize analytes with molecular weights of 10^9 Da which would correspond to extremely large-sized structures. The capability of FFF to fractionate materials of such large sizes is one of its biggest advantages over SEC.

AsFlFFF–MALS/dRI has been used to characterize starch polysaccharides and it was possible to evaluate the branching features of amylopectins and glycon [96]. Good fractionation and high mass recoveries were observed, which allowed the calculation of accurate values of radii of gyration. The same method involving programming cross-flow rate was applied to a mixture of polydisperse standard pullulans (molar size range 5.8×10^3–1.6×10^6 g/mol) [35]. Linear and exponential cross-flow decays, both with and without the initial step of constant cross-flow were applied. The results show that exponentially decaying cross-flow gave higher molar mass selectivity for the higher molar mass range.

Online coupling of field programmed frit inlet AsFlFFF with MALS has been used for the separation of high molecular weight sodium hyaluronate [97]. It was found that in order to achieve a successful separation an optimization of field programming (cross-flow rate) and experimental conditions, such as ionic strength of carrier liquid, sample concentration and injection amount should be considered.

Gelatin nanoparticles were evaluated using AsFlFFF–MALS to determine their size distribution and drug loading capacity. By developing conditions that separated the gelatin nanoparticles from an unbound model protein it was possible to determine the amount of protein that was loaded onto the gelatin nanoparticle surface through peak area comparisons [98]. A follow-up study evaluated the PEGylation of gelatin nanoparticles using AsFlFFF-dRI. The amount of PEGylation could be determined from a comparison of dRI peak areas. PEGylation is an important surface modification for gelatine nanoparticles in bio-applications because it increases the lifetime of the nanoparticle in the body, allowing it to deliver its required drug dosage [99].

Size distributions of polyelectrolyte complexes (PECs) were investigated separately by AsFlFFF and DLS. In pure

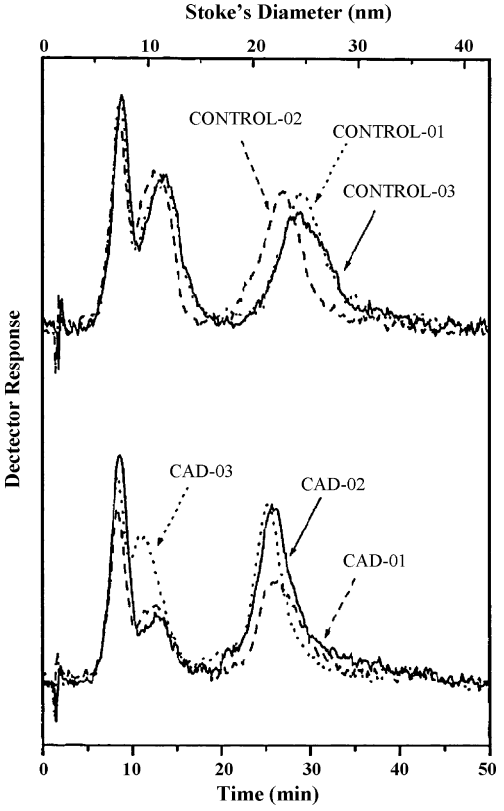

Fig. 8. AsFlFFF fractionation of HDL and LDL profiles in healthy persons (top trace) and people with known CAD (lower trace). HDL peaks appear around 10 min, and LDL peaks appear around 25 min. Reprinted from ref. [64] with permission from Elsevier.

Please cite this article in press as: Messaud FA, et al. An overview on field-flow fractionation techniques and their applications in the separation and characterization of polymers. Prog Polym Sci (2009), doi:10.1016/j.progpolymsci.2008.11.001

water, the individual anionic polymer and cationic polymer hydrodynamic diameters ranged from 20–48 nm. However, when mixed in a 1:1 ratio in salt-free deionized water, steric mode elution occurred and a bimodal distribution was observed with d_h values of ~100 nm and 2000–4000 nm. This was supported by DLS measurements of the PECs in pure deionized water. Upon addition of 20–160 mM NaCl the bimodal distribution was eliminated. The PEC nanoparticle sizes ranged from 70 to 120 nm and elution in normal mode was observed. The formation of the large, micrometer-sized particle in pure water is believed to result from PEC aggregation due to strong Coulombic interaction between charges on different particles. The number average distribution of particles was not calculated, therefore, it is possible that only a small amount of very large aggregates actually formed in pure water [79]. FlFFF is an ideal choice for this type of analyte because the integrity of the PECs, and aggregates, can be maintained in the channel due to the gentle separation of FFF.

One of the largest areas of active research in symmetric FlFFF and AsFlFFF is in the area of proteins and subcellular structures. FlFFF has been combined with MALDI-TOF–MS for the separation of intact *E. coli* and *P. putida* bacteria cells in different growth stages and the finger printing of the dominant proteins in the cell [19]. Frit inlet AsFlFFF has been shown to be a unique tool for the analysis of lipoprotein profiles in healthy persons and people with coronary artery disease (CAD) [64]. By staining blood plasma with sudan black B, the lipoproteins could be selectively identified with UV–vis detection at 610 nm without interference from plasma protein such as albumin. High density (HDL) and low density lipoproteins (LDL) were completely resolved. AsFlFFF results were used to confirm that patients with CAD had lower levels of HDL and small, more compact LDL particles than healthy patients. Fig. 8 shows the slight decrease in LDL retention time and a decrease in HDL peak intensity in patients with CAD compared to healthy patients. The easy sample preparation and short analysis time demonstrates the potential of AsFlFFF for use in clinical diagnostic settings.

AsFlFFF has been used as a high throughput screening technique to reduce the harvesting time of ribosomes from cells and to identify and relatively quantify 30S, 50S, and 70S ribosomal units. By using AsFlFFF to monitor ribosome concentrations at every step of the cell culturing, harvesting and washing process, the total ribosome analysis time was reduced from 100 to 16 min. AsFlFFF was able to fractionate ribosomes from lysed cells by direct collection of the cells from the culture, and to optimize the cell culture time by providing fast (8 min) analysis of ribosome levels every

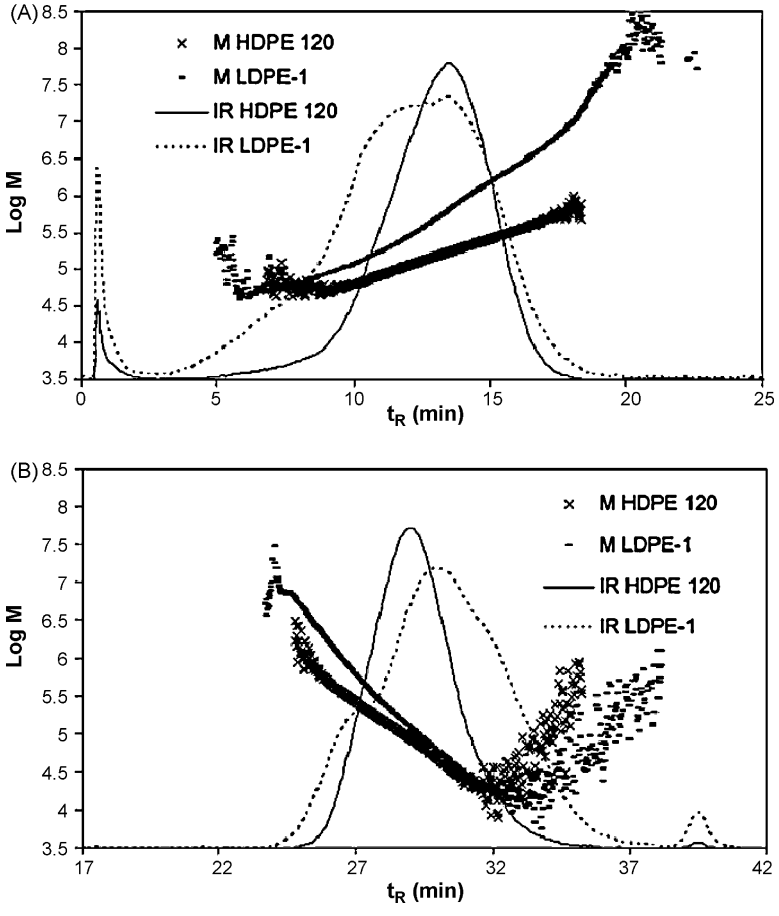

Fig. 9. Elution curves and molecular weight plots of LDPE and HDPE samples. (a) Separation with HT AsFlFFF and (b) separation with HT SEC mixed A columns. Reprinted from ref. [56] with permission from Elsevier.

Please cite this article in press as: Messaud FA, et al. An overview on field-flow fractionation techniques and their applications in the separation and characterization of polymers. Prog Polym Sci (2009), doi:10.1016/j.progpolymsci.2008.11.001

30 min during cell culture [100]. Complete resolution was observed between the 30S, 50S, and 70S ribosomes. This demonstrates the ability of FFF to be used in a bioprocess control setting.

4.2. Application of HT AsFlFFF for analyzing polyolefins

HT AsFlFFF combined with IR, MALS and viscosity detectors has been used to analyze different samples of high molecular weight high density polyethylene (HDPE) and low density polyethylene (LDPE). The measurements have been compared with the corresponding HT SEC measurements [56]. In the SEC measurements a high molecular weight shoulder appeared in the chromatogram for the LDPE samples, which was not observed in the associated fractograms (Fig. 9). The shoulder occurred as a consequence of the low size separation at the exclusion limit of the SEC column. Due to the missing separation of the high molecular weight fraction the molecular weight average and long chain branching were calculated incorrectly as seen by plotting the radius of gyration or the intrinsic viscosity versus M. Using HT AsFlFFF molecular masses up to 10^8 g/mol could be separated and characterized. In the SEC measurements such molecular weights could not be detected due to shear degradation or the size exclusion limit. The presence of shear degradation during the HT SEC measurements was verified by the comparison with offline LALS measurements.

Another phenomenon, observed in HT SEC of LDPE is the abnormal late elution of a small amount of (probably branched) high molecular weight material. The coelution of this fraction with the regularly eluting small molecules was visible as a slight upward curvature in the R_g versus M plot of LDPE in HT SEC, as shown in Fig. 10. These results demonstrate the numerous advantages of HT AsFlFFF compared with HT SEC. Once the recovery problems of the high temperature membranes are eliminated, the HT AsFlFFF should become a major tool for analyzing high molecular weight polyolefins

4.3. Thermal field-flow fractionation

Three polymer classes for which ThFFF is uniquely suited are ultrahigh molecular weight homopolymers, copolymers, and microgel-containing polymers. ThFFF is often coupled with MALS, dRI, UV–vis or viscometric detectors for absolute molecular weight or size characterization. The use of a viscometer to obtain molecular weight distributions requires knowledge of appropriate Mark-Houwink constants which are available for a variety of polymer solvent systems at different temperatures [76,101]. Combination of MALS with either a dRI or UV–vis concentration

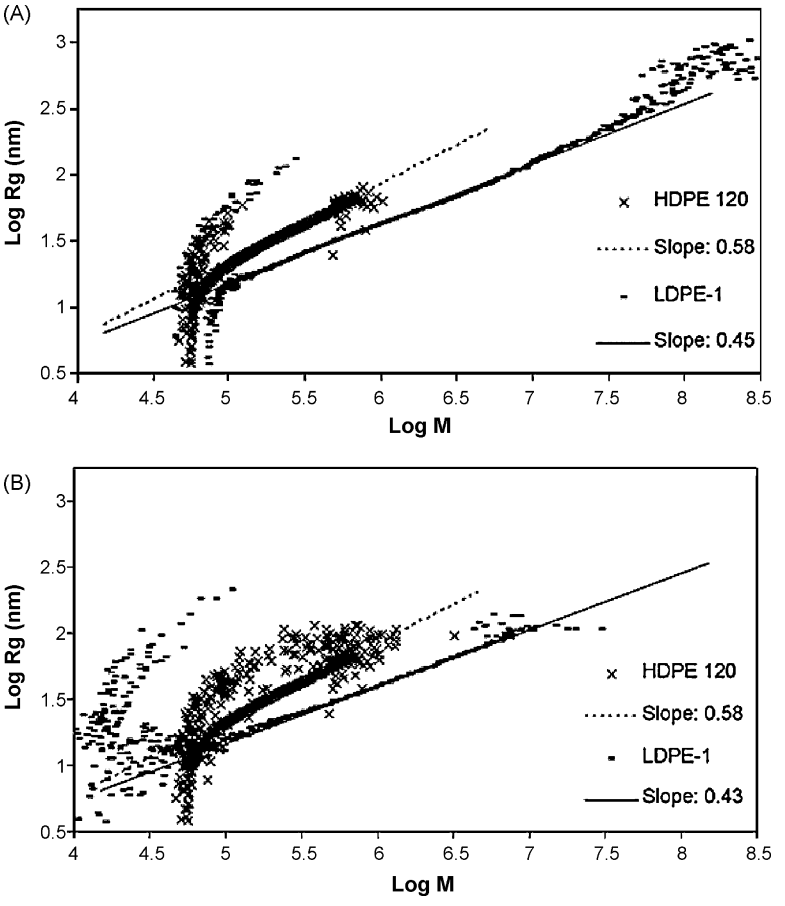

Fig. 10. Comparison of the conformation plots of HDPE and LDPE, (a) HT AsFlFFF and (b) HT SEC mixed A columns. Reprinted from ref. [56] with permission from Elsevier.

Please cite this article in press as: Messaud FA, et al. An overview on field-flow fractionation techniques and their applications in the separation and characterization of polymers. Prog Polym Sci (2009), doi:10.1016/j.progpolymsci.2008.11.001

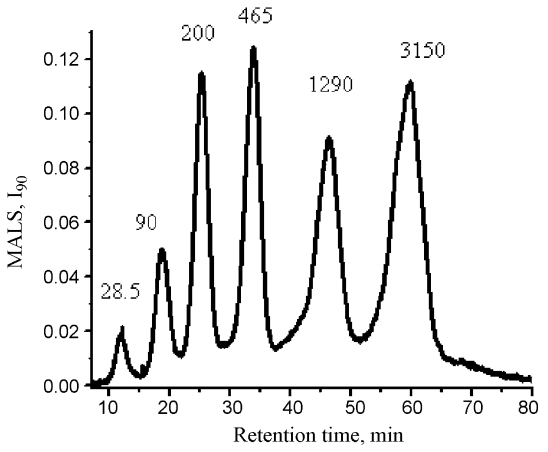

Fig. 11. Fractionation of a mixture of polystyrene standards by ThFFF. Separation conditions: programmed temperature gradient – initial ΔT: 80 °C decaying to a final ΔT of 0 °C, carrier liquid – tetrahydrofuran, flow rate: 0.1 mL/min. Peak MWs are in kDa. Work done by J. Ray Runyon, CSM.

based detector can provide absolute molecular weights and size for each slice of the eluting polymer peak.

ThFFF separation of polystyrene samples was first reported in 1969 [30]. Polystyrene standards with molecular masses ranging from 5.1×10^4 to 1.8×10^6 g/mole in tetrahydrofuran (THF) carrier were fractionated at a constant ΔT of 41 °C [77]. When a collected fraction with a nominal molar mass of 20.6×10^6 g/mole was reinjected into the ThFFF channel no significant change in elution time was observed, indicating the absence of polymer shear degradation. High resolution fractionation of a mixture of polystyrene standards across a broad molecular weight range has been accomplished in the authors' laboratory (Fig. 11). ThFFF has increased resolution and selectivity compared to SEC for polymers with molar masses greater than 100 kDa [52].

One of the advantages of ThFFF over other separation techniques that utilize a packed separation column is the upper molecular weight or size limit of the analytes that can be characterized in the open FFF channel. ThFFF has been used to analyze the microgel content of industrial polyvinyl acetate (PVAc) formulations as shown in Fig. 12 [15]. PVAc

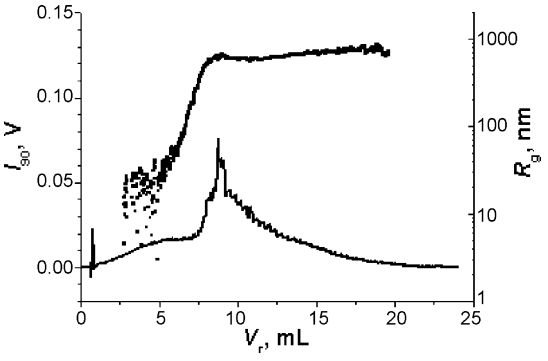

Fig. 12. ThFFF/MALS analysis of polyvinyl acetate with microgel components in the mixed solvents of dimethyl acetamide/acetonitrile 50/50 (v/v). Conditions: flow rate, 0.1 mL/min, programmed ΔT. Work done by D. Lee, CSM.

prepared under emulsion polymerization contains ultrahigh molar mass microgels due to chain-transfer reactions. The microgel components are critical to the rheological properties of the polymer. Fig. 12 shows the fractionation results of a PVAc sample used in an adhesive formulation. A programmed ΔT had to be used for the sample with broad polydispersity. The eluted components were analyzed by online MALS. The estimated radius of gyration (R_g) increased from 10 to approximately 800 nm as the elution volume increased from 2 to 20 mL. The results clearly demonstrate the ability of ThFFF to separate polymers with broad polydispersity and ultrahigh molar mass components.

ThFFF has the additional capability of separating on the basis of compositional differences. According to Eq. (15), ThFFF retention is related to the polymer's diffusion coefficient and thermal diffusion coefficient, D and D_T, respectively. The value for D_T is characteristic for different polymer–solvent systems and thus different composition polymers have different D_T values. Schimpf and Giddings conducted a broad systematic study of D_T using synthetic homopolymers in various pure organic solvents and concluded that D_T for homopolymers is independent of molecular weight and branching. Rauch and Kohler [74] extended this study by investigating low molecular weight polystyrene in toluene and found that D_T is only constant for molar masses above 10^6 g/mol in dilute solutions and decreases for lower molar masses due to end group effects. ThFFF is commonly used for synthetic polymers in organic solvents. The magnitude of D_T is low in water, which puts a limitation on the use of ThFFF for the analysis of water soluble polymers [75].

Since D_T is unique for each polymer–solvent system ThFFF has promise to measure the composition of copolymers [20,102–104]. Support for this arises from the fact that D_T values of random copolymers follow a linear trend with respect to the mole fraction of one of the constituent homopolymers, as shown for PS-co-PMMA in toluene [102]. This has also been found to be true for block copolymers in a selective solvent such as polystyrene-co-polyisoprene in THF [102]. Additionally, it has been demonstrated that D_T for copolymers is governed by radial segregation of the respective monomers, with copolymer D_T being biased towards the D_T of the monomer at the polymer-solvent interface. A mixture of 100 kDa polystyrene and 100 kDa polyvinyl-pyridine were separated with good resolution. Fig. 13 shows differences in retention times for polystyrene-co-polybutylacrylate diblock copolymers of different compositions but similar MWs (105 kDa). An increase in retention time is observed as the weight percent of polystyrene increases. This is related to the higher D_T for polystyrene ($\sim 1.6 \times 10^{-7}$ cm^2/s K in MEK) compared to polybutylacrylate ($\sim 0.8 \times 10^{-7}$ cm^2/s K in MEK). The inset in Fig. 13 shows the potential to establish calibration curves based on retention time versus weight percent of one component of the copolymer [104]. Random, diblock, and triblock polystyrene (PS)–polybutadiene (PB) copolymers with similar composition have been shown to have different retention times due to their microstructure differences [105]. These observations demonstrate that ThFFF can be used to evaluate the composition of a

Please cite this article in press as: Messaud FA, et al. An overview on field-flow fractionation techniques and their applications in the separation and characterization of polymers. Prog Polym Sci (2009), doi:10.1016/j.progpolymsci.2008.11.001

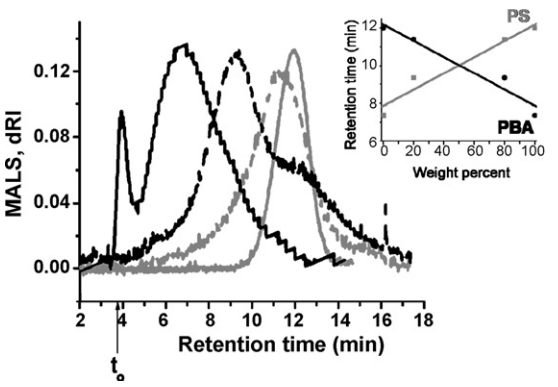

Fig. 13. ThFFF fractograms of polystyrene-co-polybutylacrylate diblock copolymers of different compositions (PBA: 100%, 80%, 20%, 0%) but similar MWs (105 kDa). Retention time differences are a result of differences in D_T for each copolymer. Conditions: carrier liquid: MEK, ΔT: 80 °C (constant), flow rate: 0.2 mL/min. Work done by J. Ray Runyon, CSM.

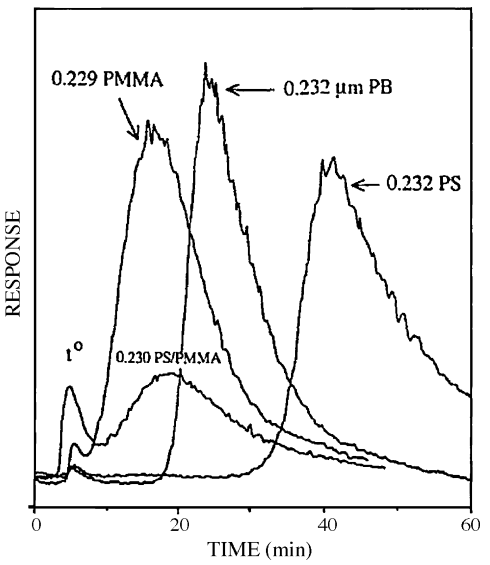

Fig. 14. Separation of particles of similar size that have different chemical composition by ThFFF. Reprinted from ref. [83] with permission from Elsevier.

copolymer by its D_T value, provided D is measured independently.

2D separations combining SEC with ThFFF have been used for the determination of the chemical composition of polydisperse samples of polymer blends and copolymers [20]. Samples of polystyrene with broad molecular mass distribution, a blend of polybutadiene, polytetrahydrofuran and polystyrene were first separated by SEC according to their size. SEC sample fractions were collected and then injected into ThFFF where separation was based on differences in D_T values. The method enabled a study of the chemical composition in each slice of the molecular mass distribution for polydisperse samples. This approach to compositional analysis is limited on the lower molar mass end by the inability of ThFFF to sufficiently retain and separate analytes below <20 kDa without extreme temperature gradients, and on the upper molecular weight end by the stationary phase in the SEC dimension. Additional examples of 2D separations involving ThFFF can be found in literature [8,103]. All of these studies have the goal of characterizing polymer molar mass and chemical composition distributions. By using a binary solvent mixture the lower molecular mass limit capability of ThFFF was reduced 10-fold to ~2.6 kDa [106].

Compositional separations by ThFFF have also been extended to polymer latex beads of similar size but different chemical composition [83]. Fig. 14 shows the different retention times for 0.232 μm polystyrene, 0.232 μm polybutadiene and 0.229 μm poly(methyl methacrylate) (PMMA). This differential retention is due to differences in the D_T values for each type of particle. Note that the 0.230 μm PS/PMMA particle has a similar retention time to 0.229 μm PMMA particle. The former is a core-shell particle, with the PMMA as the shell. This example demonstrates that ThFFF is sensitive to the surface composition of particles.

Processed natural rubber has been analyzed by field programmed ThFFF using THF solvent as a carrier liquid [80]. The determined molecular mass distribution was used to monitor the degradation of rubber during the mastication process. Additionally, the short term variability (repeatability) and long term variability (reproducibility) of ThFFF was evaluated by performing analyses over the course of several days [107]. It was found that samples differing by only 6600 Da could be resolved if analyzed on the same day, and samples differing by 15,600 Da could be resolved using the same calibration curve over the course of 4 days. This demonstrates the stability of the ThFFF instrument.

The combination of ThFFF–MALDI-TOF–MS has proven to be ideal for analyzing polymer samples with broad molar mass distributions [22,23]. This coupling addresses the limitations of each individual technique. For polydisperse samples MALDI is selective for the lower molecular mass components and the average molar mass is skewed towards this end, and polydispersity values are erroneously low. This problem is addressed by using ThFFF to fractionate the sample into more monodisperse fractions which are then collected and subjected to different optimum MALDI-TOF–MS conditions. On the other hand, the use of MALDI-TOF–MS eliminates the need to calibrate the ThFFF channel with a series of polymer standards. This work was extended by the design and implementation of an oscillating capillary nebulizer interface to directly deposit the fractionated polymer sample, together with an organic matrix, onto the MALDI sample plate in real time [23]. This greatly simplifies the ThFFF fraction collection for MALDI analysis and provides a picture of the spatial separation of the fractionated polymer. MALDI analysis at increasing times along the collected fractions showed an increasing molar mass distribution. This corroborates the elution pattern in ThFFF from lowest to highest molar mass.

ThFFF is commonly used to measure D_T values for different polymer-solvent combinations. Due to the incomplete understanding of the thermal diffusion phenomena, a predictive theory for D_T has yet to be developed. Choosing appropriate ThFFF conditions (solvent, ΔT, etc.) is traditionally a trial and error approach, which is very time consuming. This is one reason ThFFF has not experienced

Please cite this article in press as: Messaud FA, et al. An overview on field-flow fractionation techniques and their applications in the separation and characterization of polymers. Prog Polym Sci (2009), doi:10.1016/j.progpolymsci.2008.11.001

explosive growth despite its promising capabilities. Efforts have been made to predict D_T values of various polymer-solvent combinations so that appropriate ThFFF experimental conditions can be estimated. Recently, two theories have been published that show promising results and yield predicted D_T values of polystyrene of the same order of magnitude as experimental D_T values [108,109] in several different organic solvents. Ongoing work in this area will help to establish ThFFF as a major analytical tool for polymer fractionation and characterization.

5. Conclusions

FFF techniques encounter a substantial instrumental and theoretical development as well as advancement in research and applications. FlFFF and ThFFF are very capable FFF sub-techniques for fractionating synthetic, natural, and biological polymers. Each has a unique niche in polymer separations: FlFFF is more suitable to water soluble and natural polymers and ThFFF is more applicable to organosoluble polymers. However, with the recent introduction of organic compatible FlFFF systems, more applications of FlFFF to organosoluble polymers are bound to follow. When combined with MALS, dRI, UV–vis, MALDI-TOF–MS, or viscometric detection, FFF is a powerful tool for both separation and characterization of polymer molar mass distribution (MMD) and chemical composition distribution (CCD).

FFF can overcome many of the limitations of current separation techniques, especially concerning ultrahigh molecular weight analytes and microgels. For example, fractionation of the microgel content from industrial polymer formulations is possible because of the absence of a stationary phase in FFF. Therefore, FFF–MALS/dRI can provide valuable, and previously unobtainable, information about microgel content from a single sample injection. This data can be correlated with rheological measurements to determine properties of the end material.

FFF currently lacks the maturity of liquid chromatography as far as number of instruments and manufacturers, and published methods. However, as FFF continues to grow it should be viewed as a complementary technique to already established separation methods that will yield additional valuable information to gain a more global understanding of the analytes and systems in question.

Acknowledgment

JRR and SKRW gratefully acknowledge support from the National Science Foundation (CHE-0515521). RDS, FAM and HP wish to thank the Macromolecular Institute in Libya for support and M Hurndal for help in preparation.

References

[1] Pasch H. Hyphenated techniques in liquid chromatography of polymers. In: Advances in polymers science, new developments of polymer analytics. I. Berlin: Springer; 2000. p. 1–66.
[2] Philipsen HJA. Determination of chemical composition distributions in synthetic polymers. J Chromatogr A 2004;1037:329–50.
[3] Barth HG, Boyes BE, Jackson C. Size exclusion chromatography and related separation techniques. Anal Chem 1998;70:251R–78R.
[4] Glockner G. Polymer characterization by liquid chromatography. Amsterdam: Elsevier; 1987.
[5] Graef SM, Van Zyl AJP, Sanderson RD, Klumperman B, Pasch H. Use of gradient, critical and two-dimensional chromatography in the analysis of styrene and methyl methacrylate-grafted epoxidized natural rubber. J Appl Polym Sci 2003;88:2530–8.
[6] Berek D. Critical conditions and limiting conditions in liquid chromatography of synthetic polymers. Macromol Symp 2006;231:134–44.
[7] Yau W. Polyolefin microstructure characterization using 3D-GPC-TREF. TAPPI Conference, Las Vegas, NV, 2005; 19:paper 19-1.
[8] Venema E, de Leeuw P, Kraak JC, Poppe H, Tijssen R. Polymer characterization using on-line coupling of ThFFF and hydrodynamic chromatography. J Chromatogr A 1997;765:135–44.
[9] Meyers RA, editor. Encyclopedia of analytical chemistry: applications, theory, and instrumentation. Chichester: Wiley; 2000.
[10] Im K, Park HW, Kim Y, Chung B, Ree M, Chang T. Comprehensive two-dimensional liquid chromatography analysis of a block copolymer. Anal Chem 2007;79:1067–72.
[11] Myers MN. Overview of field-flow fractionation. J Microcolumn Sep 1997;9:151–62.
[12] Giddings JC. Field-flow fractionation: analysis of macromolecular, colloidal, and particulate materials. Science 1993;260:1456–66.
[13] Williams SKR, Lee D. Field-flow fractionation of proteins, polysaccharides, synthetic polymers, and supramolecular assemblies. J Sep Sci 2006;29:1720–32.
[14] Williams SKR, Benincasa MA. Field-flow fractionation analysis of polymers and rubbers. In: Meyers RA, editor. Encyclopedia of analytical chemistry: instrumentation and applications. Chichester: Wiley; 2000. p. 7582–608.
[15] Lee D, Williams SKR. Separation of ultrahigh molecular weight polymers and gels. In: 56th Pittsburgh conference on analytical chemistry and applied spectroscopy. 2005.
[16] Schimpf ME, Caldwell KD, Giddings JC, editors. Field-flow fractionation handbook. New York: Wiley; 2000.
[17] Janca J. Field-flow fractionation: analysis of macromolecules and particles. Chromatographic science series, vol. 39. NY: Marcel Dekker; 1988.
[18] Benincasa MA, Giddings JC. Separation and characterization of cationic, anionic, and nonionic water-soluble polymers by flow FFF: sample recovery, overloading, and ionic strength effects. J Microcolumn Sep 1997;9:479–95.
[19] Lee H, Williams SKR, Wahl KL, Valentine NB. Analysis of whole bacterial cells by flow field-flow fractionation and matrix-assisted laser desorption/ionization time-of-flight mass spectrometry. Anal Chem 2003;75:2746–52.
[20] van Asten AC, van Dam RJ, Kok WTh, Tijssen R, Poppe H. Determination of the compositional heterogeneity of polydisperse polymer samples by coupling of size exclusion chromatography and thermal field-flow fractionation. J Chromatogr A 1995;703:245–63.
[21] Jagtap R, Ambre H. Overview literature on matrix assisted laser desorption ionization mass spectroscopy (MALDI MS): basics and its applications in characterizing polymeric materials. Bull Mater Sci 2005;28:515–28.
[22] Pasch H, Schrepp W. MALDI-TOF mass spectrometry of synthetic polymers. Berlin: Springer; 2003.
[23] Basile F, Kassalainen GE, Williams SKR. Interface for direct and continuous sample-matrix deposition onto a MALDI probe for polymer analysis by thermal field-flow fractionation and off-line MALDI-MS. Anal Chem 2005;77:3008–12.
[24] Giddings JC. A new separation concept based on a coupling of concentration and flow nonuniformities. J Sep Sci 1966;1:123–5.
[25] Chmelik J. Different elution modes and field programming in gravitational field-flow fractionation: A theoretical approach. J Chromatogr A 1999;845:285–91.
[26] Giddings JC, Myers MN. Steric field-flow fractionation: a new method for separating 1–100 μm particles. Sep Sci Technol 1978;13:637–45.
[27] Caldwell KD, Nguyen TT, Myers MN, Giddings JC. Observations on anomalous retention in steric field-flow fractionation. Sep Sci Technol 1979;14:935–46.
[28] Giddings JC. Hyperlayer field-flow fractionation. Sep Sci Technol 1983;18:765–73.
[29] Beckett R, Sharma R, Andric G, Chantiwas R, Jakmunee J, Grudpan K. Illustrating some principles of separation science through gravitational field-flow fractionation. J Chem Educ 2007;84:1955–62.
[30] Carpino F, Moore LR, Zborowski M, Chalmers JJ, Williams PS. Analysis of magnetic nanoparticles using quadrupole magnetic field-flow fractionation. J Magn Magn Mater 2005;293:546–52.

Please cite this article in press as: Messaud FA, et al. An overview on field-flow fractionation techniques and their applications in the separation and characterization of polymers. Prog Polym Sci (2009), doi:10.1016/j.progpolymsci.2008.11.001

[31] Semyonov SN, Maslow KI. Acoustic field-flow fractionation. J Chromatogr 1988;446:151–6.
[32] Moon MH, Williams PS, Kang D, Hwang I. Field and flow programming in frit inlet asymmetrical flow field-flow fractionation. J Chromatogr A 2002;955:263–72.
[33] Williams PS, Giddings JC. Theory of field programming field-flow fractionation with corrections for steric effects. Anal Chem 1994;66:4215–28.
[34] Williams PS, Giddings MC, Giddings JC. A data analysis algorithm for programmed field-flow fractionation. Anal Chem 2001;73:4202–11.
[35] Leeman M, Wahlund KG, Wittgren B. Programmed cross flow asymmetrical flow field-flow fractionation for the size separation of pullulans and hydroxypropyl cellulose. J Chromatogr A 2006;1134:236–45.
[36] Wahlund KG, Giddings JC. Properties of an asymmetrical flow field-flow fractionation channel having one permeable wall. Anal Chem 1987;59:1332–9.
[37] Litzen A. Separation speed, retention, and dispersion in asymmetrical flow field-flow fractionation as functions of channel dimensions and flow rates. Anal Chem 1993;65:461–70.
[38] Williams PS. Design of asymmetric flow field-flow fractionation channel for uniform channel flow velocity. J Microcolumn Sep 1997;9:459–67.
[39] Park I, Paeng KJ, Kang D, Moon MH. Performance of hollow-fiber flow field-flow fractionation in protein separation. J Sep Sci 2005;28:2043–9.
[40] Se-Jong S, Hyun-Hee N, Byoung-Ryul M, Jin-Won P, Ik-Sung A, Kangtaek L. Separation of proteins mixtures in hollow fiber flow field-flow fractionation. Bull Korean Chem Soc 2003;24:1339–44.
[41] Kang D, Moon MH. Miniaturization of frit-inlet AsFlFFF. Anal Chem 2004;76:3851–5.
[42] Sant HJ, Gale BK. Geometric scaling effects on instrumental plate height in field flow fractionation. J Chromatogr A 2006;1104:282–90.
[43] Yohannes G, Sneck M, Varjo SJO, Jussila M, Wiedmer SK, Kovanen PT, Oorni K, Riskily ML. Miniaturization of asymmetric flow field-flow fractionation and application to studies on lipoprotein aggregation and fusion. Anal Biochem 2006;354:255–65.
[44] Janca J. Microthermal field-flow fractionation: analysis of synthetic, natural, and biological macromolecules and particles. New York: HNB Publishing; 2008.
[45] Janca J, Ananieva IA. Micro-thermal field-flow fractionation in the characterization of macromolecules and particles: effect of the steric exclusion mechanism. E-Polymers 2003; Paper no. 034.
[46] Edwards TL, Gale BK, Frazier AB. A microfabricated thermal field-flow fractionation system. Anal Chem 2002;74:1211–6.
[47] Bargiel S, G-Drzazga A, Dziuban J. A micromachined system for the separation of molecules using ThFFF method. Diss Abstr Int 2005:66.
[48] Janca J. Micro-channel thermal field-flow fractionation: new challenge in analysis of macromolecules and particles. J Liq Chromatogr Rel Technol 2002;25:683–704.
[49] Janca J. Micro-channel thermal field-flow fractionation: analysis of ultra-high molar mass polymers and colloidal particle with constant and programmed field force operation. J Liq Chromatogr Rel Technol 2003;26:2173–91.
[50] Janca J. Micro-channel thermal field-flow fractionation: high speed analysis of colloidal particles. J Liq Chromatogr Rel Technol 2003;26:849–69.
[51] Giddings JC, Yang FJ, Myers MN. Theoretical and experimental characterization of flow field-flow fractionation. Anal Chem 1976;48:1126–32.
[52] Gunderson JJ, Giddings JC. Comparison of polymer resolution in thermal field-flow fractionation and size-exclusion chromatography. Anal Chim Acta 1986;189:1–15.
[53] Li P, Hanson M, Giddings JC. Advances in frit-inlet and frit-outlet flow field-flow fractionation. J Microcolumn Sep 1997;10:7–18.
[54] Giddings JC, Yu X, Myers MN. Enhancement of performance in sedimentation field-flow fractionation by temperature elevation. Anal Chem 1994;66:3047–53.
[55] Stegeman G, van Asten AC, Kraak JC, Poppe H, Tijssen R. Comparison of resolving power and separation time in thermal field-flow fractionation, hydrodynamic chromatography, and size-exclusion chromatography. Anal Chem 1994;66:1147–60.
[56] Mes EPC, de Jonge H, Klein T, Welz RR, Gillespie DT. Characterization of high molecular weight polyethylenes using high temperature asymmetric flow field-flow fractionation with on-line infrared, light scattering and viscometry detection. J Chromatogr A 2007;1154:319–30.
[57] Leeman M, Islam MT, Haseltine WG. Asymmetric flow field-flow fractionation coupled with multiangle light scattering and refractive index detectors for characterization of ultra-high molar mass poly(acrylamide) flocculants. J Chromatogr A 2007;1172:194–203.
[58] Sisson RM, Giddings JC. Effects of solvent composition on polymer retention in thermal field-flow fractionation: Retention enhancement in binary solvent mixtures. Anal Chem 1994;66:4043–53.
[59] Belgaied JE, Hoyos M, Martin M. Velocity profiles in thermal field-flow fractionation. J Chromatogr A 1994;678:85–96.
[60] Lee S. Application of thermal field-flow fractionation for characterization of industrial polymers. J Microcolumn Sep 1997;9:281–6.
[61] Pasti L, Melluci D, Contado C, Dondi F, Mingozzi I. Calibration in thermal field-flow fractionation with polydisperse standards: application to polyolefin characterization. J Sep Sci 2002;25:691–701.
[62] Cao W, Williams PS, Meyers MN, Giddings JC. Thermal field-flow fractionation universal calibration: extension for consideration of cold wall temperature. Anal Chem 1999;71:1597–609.
[63] Kang D, Sunok O, Reschiglian P, Moon MH. Separation of mitochondria by flow field-flow fractionation for proteomic analysis. Analyst 2008;133:505–15.
[64] Park I, Paeng KJ, Yoong Y, Song JH, Moon MH. Separation and selective detection of lipoprotein particles of patients with coronary artery disease by frit-inlet asymmetrical flow field-flow fractionation. J Chromatogr B 2002;780:415–22.
[65] Wittgren B, Wahlund KG. Fast molecular and size characterization of polysaccharides using asymmetrical field-flow fractionation-multiangle light scattering. J Chromatogr A 1997;760:205–18.
[66] Salesse C, Battu S, Begaud-Grimud G, Cledat D, Cook-Moreau J, Cardot PJP. Sedimentation field-flow fractionation monitoring of bimodal wheat starch amylolysis. J Chromatogr A 2006;1129:247–54.
[67] Daval C, Le Cerf D, Picton L, Muller G. Aggregation of amphiphilic pullulan derivatives evidenced by online flow field-flow fractionation multi-angle laser light scattering. J Chromatogr B 2001;753:115–22.
[68] Picton L, Bataille I, Muller G. Analysis of a complex polysaccharide (gum arabic) by multi-angle laser light scattering coupled on-line to size exclusion chromatography and flow field-flow fractionation. Carbohyd Polym 2000;42(1):23–31.
[69] Anderson M, Wittgren B, Wahlund KG. Ultrahigh molar mass component detected in ethylhydroxyethyl cellulose by asymmetrical field-flow fractionation coupled to multiangle light scattering. Anal Chem 2001;73:4852–61.
[70] Lee S, Nilsson PO, Nilson GS, Wahlund KG. Development of asymmetrical flow field-flow fractionation-multiangle laser light scattering analysis for molecular mass characterization of cationic potato amylopectin. J Chromatogr A 2003;1011:111–23.
[71] Van Bruijnsvoort M, Wahlund KG, Nilsson G, Kok WTh. Retention behavior of amylopectins in asymmetric flow field-flow fractionation studied by multiangle light scattering detection. J Chromatogr A 2001;925:171–82.
[72] Farmakis L, Koliadima A, Karaiskakis G, Zattoni A, Reschiglian P. Study of the influence of surfactants on the size distribution and mass ratio of wheat starch granules by sedimentation/steric field-flow fractionation. Food Hydrocolloids 2008;22:961–72.
[73] Wittgren B, Wahlund KG. Effects of flow rates and sample concentration on the molar mass characterization of modified cellulose using asymmetric flow field-flow fractionation-multi-angle light scattering. J Chromatogr A 1997;791:135–49.
[74] Rauch J, Kohler W. On the molar mass dependence of the thermal diffusion coefficient of polymer solutions. Macromolecules 2005;38:3571–3.
[75] Dammert R, Jussila M, Vastamaki P, Riekkola ML, Sundholm F. Determination and comparison of molar mass distribution of substituted polystyrenes and block copolymers by using thermal field-flow fractionation, size exclusion chromatography and light scattering. Polymer 1997;38:6273–80.
[76] Kirkland JJ, Rementer SW. Polymer molecular weight distributions by thermal field-flow fractionation using Mark-Houwink constants. Anal Chem 1992;64:904–13.
[77] Gao YS, Caldwell KD, Myers MN, Giddings JC. Extension of thermal field-flow fractionation to ultrahigh molecular weight polystyrenes. Macromolecules 1985;18:1272–7.
[78] Kassalainen GE, Williams SKR. Coupling thermal field-flow fractionation with matrix-assisted laser desorption/ionization time-of-flight mass spectrometry for the analysis of synthetic polymers. Anal Chem 2003;75:1887–94.

Please cite this article in press as: Messaud FA, et al. An overview on field-flow fractionation techniques and their applications in the separation and characterization of polymers. Prog Polym Sci (2009), doi:10.1016/j.progpolymsci.2008.11.001

[79] Yohannes G, Holappa S, Wiedmer SK, Andersson T, Tenhu H, Riekkola ML. Polyelectrolyte complexes of poly-(methacryloxyethyl trimethylammonium chloride) and poly(ethylene oxide)-block-poly(sodium methacrylate) studied by asymmetrical flow field-flow fractionation and dynamic light scattering. Anal Chim Acta 2005;542:222–9.
[80] Lee S, Eun CH, Plepys AR. Capability of thermal field-flow fractionation for analysis of processed natural rubber. Bull Korean Chem Soc 2000;21:69–74.
[81] Frankema W, van Bruijnsvoort M, Tijssen R, Kok WTh. Characterization of core-shell latexes by flow field-flow fractionation with multi-angle light scattering detection. J Chromatogr A 2002;943:251–61.
[82] Vastamaki P, Jussila M, Riekkola ML. Continuous two-dimensional field flow fractionation: a novel technique for continuous separation and collection of macromolecules and particles. Analyst 2005;130:427–32.
[83] Shiundu PM, Giddings JC. Influence of bulk and surface composition on the retention of colloidal particles in thermal field flow fractionation. J Chromatogr A 1995;715:117–26.
[84] Shiundu PM, Munguti SM, Williams SKR. Practical implications of ionic strength effects on particle retention in thermal field-flow fractionation. J Chromatogr A 2003;984:67–79.
[85] Giddings JC. Factors influencing accuracy of colloids and macromolecules properties measured by field-flow fractionation. Anal Chem 1997;69:552–7.
[86] Gimbert LJ, Andrew KN, Haygarth PM, Worsfold PJ. Environmental applications of flow field-flow fractionation. Trends Anal Chem 2003;22:615–33.
[87] Moon J, Kim SJ, Cho J. Characterization of natural organic matter as nano-particles using flow field-flow fractionation. Colloids Surf A 2006;287:232–6.
[88] Dycus PJM, Healy KD, Stearman GK, Wells MJM. Diffusion coefficients and molecular weight distributions of humic and fulvic acids determined by flow field-flow fractionation. Sep Sci Technol 1995;30:1435–53.
[89] Siripinyanond A, Barnes RM. Flow field-flow fractionation-inductively coupled plasma mass spectrometry of chemical mechanical polishing slurries. Spectrochim Acta Part B 2002;57:1885–96.
[90] Bohner M, Ring TA, Rapoport N, Caldwell KD. Fibrinogen uptake by PS latex particles coated with various amounts of a PEO/PPO/PEO triblock copolymer. J Biomater Sci Polym E 2002;13:732–45.
[91] Hartmann RL, Williams SKR. Flow field-flow fractionation as an analytical technique to rapidly quantitate membrane fouling. J Membr Sci 2002;209:93–106.
[92] Bang DY, Shin DY, Lee S, Moon MH. Characterization of functionalized styrene-butadiene rubber by flow field-flow fractionation/light scattering in organic solvent. J Chromatogr A 2007;1147:200–5.
[93] Thielking H, Clicked WM. On-line coupling of flow field-flow fractionation and multiangle laser light scattering for the characterization of macromolecules in aqueous solution as illustrated by sulfonated polystyrene samples. Anal Chem 1996;68:1169–73.
[94] Moon MH, Kwon H, Park I. Stoppless flow injection in asymmetrical flow field-flow fractionation using a frit inlet. Anal Chem 1997;69:1436–40.
[95] Yohannes G, Shan J, Jussila M, Nuopponea M, Tenhu H, Riekkola ML. Characterization of poly(*N*-isopropylacrylamide) by asymmetrical flow field-flow fractionation, dynamic light scattering, and size exclusion chromatography. J Sep Sci 2005;28:435–42.
[96] Rolland-Sabate A, Colonna P, Mendez-Montealvo MG, Planchot V. Branching features of amylopectins and glycon determined by asymmetrical flow field-flow fractionation coupled with multiangle laser light scattering. Biomacromolecules 2007;8:2520–32.
[97] Lee H, Kim H, Moon MH. Field programming in frit-inlet asymmetrical flow field-flow fractionation/multiangle light scattering: application to sodium hyaluronate. J Chromatogr A 2005;1089:203–10.
[98] Fraunhofer W, Winter G, Coester C. Asymmetrical flow field-flow fractionation and multiangle light scattering for analysis of gelatin nanoparticle drug carrier systems. Anal Chem 2004;76:1909–20.
[99] Zillies JC, Zwiorek K, Winter G, Coester C. Method for quantifying the PEGylation of gelatin nanoparticle drug carrier systems using asymmetrical flow field-flow fractionation and refractive index detection. Anal Chem 2007;79:4574–80.
[100] Arfvidsson C, Wahlund KG. Time-minimized determination of ribosome and tRNA levels in bacterial cells using flow field-flow fractionation. Anal Biochem 2003;313:76–85.
[101] Schimpf ME, Giddings JC. Characterization of thermal diffusion of copolymers in solution by thermal field-flow fractionation. J Polym Sci Part B: Polym Phys 1990;28:2673–80.
[102] Schimpf ME, Wheeler LM, Romeo PF. Copolymer retention in thermal field-flow fractionation: dependence on composition and conformation. Chromatography of polymers: characterization by SEC and FFF, vol. 521. Washington, DC: ACS Symposium Series; 1993. pp. 63–76.
[103] Jeon S, Schimpf ME. Cross-fractionation of copolymers using SEC and Thermal FFF for determination of molecular weight and composition. Chromatography of polymers: hyphenated and multidimensional techniques, vol. 731. Washington, DC: ACS Symposium Series; 2000. pp. 141–161.
[104] Runyon JR, Williams SKR. Thermal field-flow fractionation of acrylic copolymers. In: 13th International Symposium on Field- and Flow-based Separations. 2007 June.
[105] Williams SKR. Addressing new challenges in polymer analysis using field-flow fractionation and MALDI-MS. In: Macro 2006-41st International Symposium on Macromolecules Proceedings. 2006.
[106] Kassalainen GE, Williams SKR. Lowering the molecular mass limit of thermal field-flow fractionation for polymer separations. J Chromatogr A 2003;988:285–95.
[107] Kim WS, Eun CH, Molnar A, Yu JS, Lee S. Repeatability and reproducibility of thermal field-flow fractionation in molecular weight determination of processed natural rubber. Analyst 2006;131:429–33.
[108] Schimpf ME, Semenov SN. Polymer thermophoresis in solvents and solvent mixtures. Phil Magn 2003;83:2185–98.
[109] Mes EPC, Kok WTh, Tijssen R. Prediction of polymer thermal diffusion coefficients from polymer-solvent interaction parameters: comparison with thermal field-flow fractionation and thermal diffusion forced Rayleigh scattering experiments. Int J Polym Anal and Charac 2003;8:133–53.

Please cite this article in press as: Messaud FA, et al. An overview on field-flow fractionation techniques and their applications in the separation and characterization of polymers. Prog Polym Sci (2009), doi:10.1016/j.progpolymsci.2008.11.001